

# Magnetic coupling between $A'$ and $B$ sites in the $A$ -site-ordered perovskite $\text{BiCu}_3\text{Mn}_4\text{O}_{12}$

Takashi Saito (齊藤高志),<sup>1,\*</sup> Wei-tin Chen (陳威廷),<sup>1,2</sup> Masaichiro Mizumaki (水牧仁一朗),<sup>3</sup> J. Paul Attfield,<sup>2</sup> and Yuichi Shimakawa (島川祐一)<sup>1</sup>

<sup>1</sup>*Institute for Chemical Research, Kyoto University, Gokasho, Uji, Kyoto 611-0011, Japan*

<sup>2</sup>*Centre for Science at Extreme Conditions and School of Chemistry, University of Edinburgh, Mayfield Road, Edinburgh EH9 3JZ, United Kingdom*

<sup>3</sup>*Japan Synchrotron Radiation Research Institute, 1-1-1 Kouto, Sayo-cho, Sayo-gun, Hyogo 679-5198, Japan*  
(Received 18 February 2010; revised manuscript received 7 June 2010; published 26 July 2010)

The ionic states of Cu and Mn ions and the magnetic structure in an  $A$ -site-ordered perovskite  $\text{BiCu}_3\text{Mn}_4\text{O}_{12}$  were investigated by powder neutron diffraction and soft x-ray absorption and magnetic circular dichroism spectroscopy experiments. A substitution by  $\text{Mn}^{3+}$  was found at the square-planar  $A'$   $\text{Cu}^{2+}$  site, leading to a composition  $\text{Bi}(\text{Cu}_{0.8}^{2+}\text{Mn}_{0.2}^{3+})_3\text{Mn}_{3.6}^{3+}\text{O}_{12}$ . This compound is a ferrimagnet with a collinear spin configuration below  $T_C=350$  K, and the magnetic structure is stabilized by a strong ferromagnetic coupling between the  $A'$  and  $B$  site Mn ions and an antiferromagnetic coupling between Cu and Mn ions, leading to a near zero net moment at the  $A'$  site.

DOI: 10.1103/PhysRevB.82.024426

PACS number(s): 75.25.-j, 75.47.-m, 71.30.+h

## I. INTRODUCTION

Perovskite oxides containing transition metal (TM) ions at the  $A$  site of the  $\text{ABO}_3$  structure are quite rare. This is mainly because TM ions are too small to be stabilized at the usually 12-fold  $A$  site. However, particular types of distortions in the  $\text{BO}_6$  octahedron network produce quasisquare-planar coordination at some part of the  $A$  sites that can incorporate Jahn-Teller (JT) active TM ions.<sup>1</sup> An example of such an  $A$ -site-ordered perovskite is  $AA'_3B_4\text{O}_{12}$ , in which 3/4 of the  $A$  sites in an  $\text{ABO}_3$  perovskite (denoted as the  $A'$  site) are occupied by JT ions such as  $\text{Cu}^{2+}$  and  $\text{Mn}^{3+}$ , with a  $2a_0 \times 2a_0 \times 2a_0$  cubic unit cell of  $Im-3$  symmetry ( $a_0$ : lattice constant of the perovskite prototype), as illustrated in Fig. 1. The presence of the TM ions at the  $A'$  sites is expected to induce  $A'-A'$  and  $A'-B$  interactions as well as the  $B-B$  interaction seen in many perovskite oxides, which give rise to novel physical properties in the  $AA'_3B_4\text{O}_{12}$  compounds.

Compounds with this characteristic structure show wide variety of properties. Cu  $3d$  electrons in the insulating  $\text{CaCu}_3B_4\text{O}_{12}$  ( $B=\text{Ti, Ge, Sn}$ ) are localized as  $A'$ -site  $S=1/2$  spins.  $\text{CaCu}_3\text{Ti}_4\text{O}_{12}$  exhibits temperature-independent colossal dielectric constant<sup>2</sup> and the  $B=\text{Ge, Sn}$  materials are very rare ferromagnetic cuprates.<sup>3</sup> For compounds with Ru or V at the  $B$  site, in contrast, Cu  $3d$  electrons are itinerant and the materials show metallic behavior.<sup>4,5</sup> Metallic  $\text{CaCu}_3\text{Ru}_4\text{O}_{12}$  is reported to exhibit a heavy-fermionlike behavior without  $f$  electrons.<sup>4</sup>  $\text{CaCu}_3\text{Mn}_4\text{O}_{12}$  is a ferrimagnet with a Curie temperature above room temperature, and its ferrimagnetism is explained by a ferrimagnetic ordering of the  $A'$ -site Cu and  $B$ -site Mn spins.<sup>6</sup> Conduction carriers doped by substituting  $\text{La}^{3+}$  or  $\text{Bi}^{3+}$  for  $\text{Ca}^{2+}$  induce metallic conductivity and a large magnetoresistance effect at very low magnetic fields.<sup>7,8</sup> A first-principles band-structure calculation revealed that the substitution caused mixed valence states in Mn in  $\text{LaCu}_3\text{Mn}_4\text{O}_{12}$  and  $\text{BiCu}_3\text{Mn}_4\text{O}_{12}$ , leading to half metallic states.

In this paper, we have examined the ionic states of Cu and Mn ions in  $\text{BiCu}_3\text{Mn}_4\text{O}_{12}$  and their magnetic interaction.

Soft x-ray absorption and magnetic circular dichroism spectroscopy (XAS-MCD) gave a direct evidence of antiferromagnetic coupling between the  $A'$ -site Cu and  $B$ -site Mn spins. We will also discuss the magnetic structure of the compound from the analysis of neutron powder-diffraction (NPD) data.

## II. EXPERIMENTS

A polycrystalline sample of  $\text{BiCu}_3\text{Mn}_4\text{O}_{12}$  was prepared using a high-pressure technique, as described in Ref. 8. The obtained sample was almost single phase but it included a small amount of CuO impurity. As shown in Fig. 2, a large magnetization of the sample at low temperature was confirmed by a superconducting quantum interference device magnetometer (Quantum Design, magnetic property measurement system) measurement. The magnetic transition temperature  $T_C$  determined from the magnetic susceptibility data in a magnetic field of 0.1 T was 350 K. Assuming the stoichiometric composition, saturation magnetization of  $10.6 \mu_B/\text{f.u.}$  was obtained in a magnetic field of 5 T at 5 K, in good agreement with the previous report.<sup>8</sup>

The XAS-MCD measurements at the Cu  $L_{2,3}$  and Mn  $L_{2,3}$  edges were carried out at 9 K, by a total electron yield

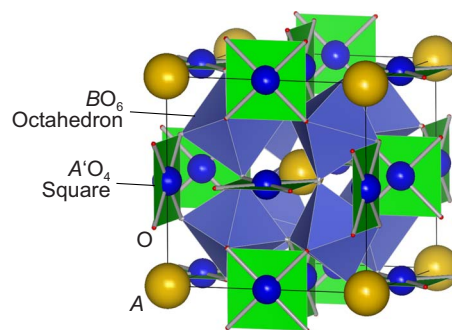


FIG. 1. (Color online) Crystal structure of the  $A$ -site-ordered perovskite  $AA'_3B_4\text{O}_{12}$ .

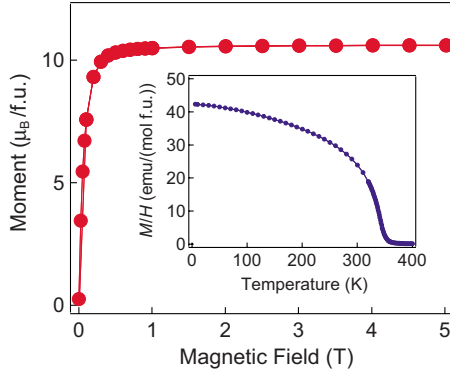


FIG. 2. (Color online) Isothermal magnetization of BiCu<sub>2.4</sub>Mn<sub>4.6</sub>O<sub>12</sub> at 5 K and the temperature dependence of the dc magnetic susceptibility in a magnetic field of 0.1 T (inset), both assuming stoichiometric composition. The saturation magnetization was corrected to be 12.1  $\mu_B$ /f.u. considering the off-stoichiometry, as described in the text.

method at the soft x-ray beamline BL25SU of SPring-8 in Japan. The energy resolution  $E/\Delta E$  was greater than 5000 during the measurements. The incident photon energy was calibrated by measuring the energies of the Ti  $L_{2,3}$  edges of TiO<sub>2</sub> and the Ni  $L_{2,3}$  edges of NiO. Powder sample was pasted uniformly on a sample holder by using a carbon tape, and a magnetic field of 2 T was applied during the measurement. The MCD was obtained by altering the direction of the magnetic field with respect to the spin of the circularly polarized soft x-ray. The MCD spectrum is defined as  $I_+ - I_-$ , where  $I_+$  and  $I_-$  represent the absorption intensity with the direction of the magnetization being parallel and antiparallel to the photon spin, respectively.

NPD patterns were collected in the temperature range from 5 to 400 K on the high-resolution D2B diffractometer of the Institute Laue-Langevin in Grenoble. About 1 g of powder sample was used and good quality patterns were collected with the high-flux mode. The counting time was 6 h for the 400 and 5 K patterns, and 4 h for the rest. A wavelength of 1.594 Å was used and the data were analyzed by the Rietveld method, using the program GSAS.<sup>9</sup>

### III. RESULTS AND DISCUSSION

The NPD patterns above  $T_C$  were well reproduced with an A-site-ordered structure model with a space group  $Im\bar{3}$ . Here Bi atoms were placed at  $2a$  (0,0,0) positions, Cu at  $6b$  (0, 1/2, 1/2) ( $A'$  site), Mn at  $8c$  (1/4, 1/4, 1/4) ( $B$  site), and O at  $24g$  (0,  $y$ ,  $z$ ). The result of the Rietveld refinement at 400 K is shown in Fig. 3 and the refined parameters are listed in Table I. The fit improved considerably with a reduction in  $R_{wp}$  from 6.25% to 4.96%, by partially incorporating Mn at the  $A'$  site. Incorporating Cu at the  $B$  site in the refinement did not give significant improvement. We note that the coherent neutron-scattering length of Mn is negative (−3.73 fm) while that of Cu is positive (7.69 fm) so that neutron diffraction is very sensitive for distinguishing Mn and Cu. Oxygen vacancies were not detected in the refinement of the oxygen site occupancy. Thus, the

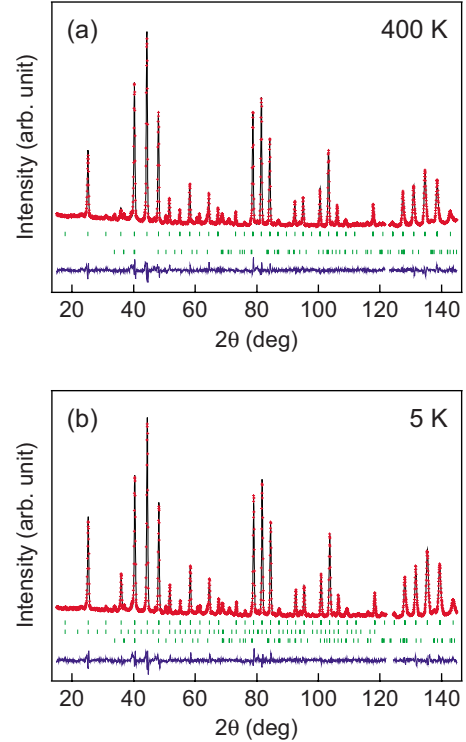


FIG. 3. (Color online) Observed (+), calculated (full line), and difference (bottom) NPD Rietveld profiles for BiCu<sub>2.4</sub>Mn<sub>4.6</sub>O<sub>12</sub> at (a) 400 K and (b) 5 K. The bottom row of tick marks corresponds to the small CuO impurity in both patterns and the middle row at 5 K corresponds to the magnetic structure.

obtained chemical formula was Bi(Cu<sub>0.8</sub>Mn<sub>0.2</sub>)<sub>3</sub>Mn<sub>4</sub>O<sub>12</sub> (BiCu<sub>2.4</sub>Mn<sub>4.6</sub>O<sub>12</sub>). The additional Mn<sup>3+</sup> included in this compound is also a JT ion, and is known to be incorporated into the  $A'$  site, as in NaMn<sub>3</sub>Mn<sub>4</sub>O<sub>12</sub> or LaMn<sub>3</sub>Cr<sub>4</sub>O<sub>12</sub>.<sup>10,11</sup> Such off-stoichiometry is also reported in CaCu<sub>3</sub>Mn<sub>4</sub>O<sub>12</sub>.<sup>12</sup> The off-stoichiometry is also consistent with the observations of CuO (5.7 wt %) and Bi<sub>2</sub>(CO<sub>3</sub>)O<sub>2</sub> impurities<sup>8</sup> detected in the present neutron and x-ray (data is not shown) diffraction data. Assuming JT active Cu<sup>2+</sup> and Mn<sup>3+</sup> at the square-planar coordinated  $A'$  site, the refined chemical composition gives a nominal valence of 3.6+ for Mn at the  $B$  site (Mn<sub>B</sub>). The oxidation states of the cations in BiCu<sub>2.4</sub>Mn<sub>4.6</sub>O<sub>12</sub> were also assessed by means of Brown's bond valence sum (BVS) calculation,<sup>13</sup> using the observed metal-oxygen distances at room temperature. No structural transition was observed at magnetic  $T_C$  and the cubic  $Im\bar{3}$  crystal structure was kept intact below  $T_C$ . The refined structural parameters at 300 K are listed in Table I, and selected bond distances and bond angles are listed in Table II. The BVS calculated from the bond distances were 2.22 for Cu<sub>A'</sub> and 2.76 for Mn<sub>A'</sub> (both based on the average Cu<sub>A'</sub>/Mn<sub>A'</sub>-O distances), 3.61 for Mn<sub>B</sub>, and 3.12 for Bi. The results are fully consistent with the nominal composition Bi<sup>3+</sup>(Cu<sup>2+</sup><sub>0.8</sub>Mn<sup>3+</sup><sub>0.2</sub>)<sub>3</sub>Mn<sup>3.6+</sup><sub>4</sub>O<sub>12</sub>. (The small deviation of the BVS for Cu<sub>A'</sub>/Mn<sub>A'</sub> from 2+/3+ should come from the usage of the average atomic distances.)

The ionic states of the  $A'$ -site Cu ions and the  $B$ -site Mn ions and their magnetic coupling were also examined in detail with XAS-MCD measurements. The Cu and

TABLE I. Representative refined structural parameters of BiCu<sub>2.4</sub>Mn<sub>4.6</sub>O<sub>12</sub> at 400, 300, and 5 K.<sup>a</sup>

		400 K <sup>b</sup>	300 K	5 K
<i>a</i> (Å)		7.33130(8)	7.32352(8)	7.31188(7)
<i>V</i> (Å <sup>3</sup> )		394.04(1)	392.79(1)	390.92(1)
Bi	<i>U</i> <sub>iso</sub> (Å <sup>2</sup> )	0.020(1)	0.018(1)	0.0109(9)
Cu/Mn	Cu occupancy	0.800(4)	0.8	0.8
	Mn occupancy	0.200(4)	0.2	0.2
Mn	<i>U</i> <sub>iso</sub> (Å <sup>2</sup> )	0.0089(6)	0.0077(5)	0.0045(4)
	Magnetic moment (μ <sub>B</sub> )	0	0	0.24(4)
	<i>U</i> <sub>iso</sub> (Å <sup>2</sup> )	0.0098(5)	0.0096(6)	0.0068(5)
O	Magnetic moment (μ <sub>B</sub> )	0	1.60(9)	2.86(5)
	<i>y</i>	0.3046(2)	0.3046(2)	0.3044(2)
	<i>z</i>	0.1810(2)	0.1807(2)	0.1808(2)
	<i>U</i> <sub>iso</sub> (Å <sup>2</sup> )	0.0103(2)	0.0092(2)	0.0059(2)
<i>R</i> <sub>wp</sub> (%)		4.96	4.89	5.55
<i>R</i> <sub>p</sub> (%)		3.45	3.69	3.80
χ <sup>2</sup>		4.65	3.77	5.33

<sup>a</sup>Cubic space group *Im-3* (No, 204) was adopted for all the crystal structural refinements, where the atomic positions were Bi 2*a* (0,0,0)(*A* site), Cu/Mn 6*b* (0,  $\frac{1}{2}$ ,  $\frac{1}{2}$ )(*A'* site), Mn 8*c* ( $\frac{1}{4}$ ,  $\frac{1}{4}$ ,  $\frac{1}{4}$ )(*B* site), and O 24*g* (0, *y*, *z*).

<sup>b</sup>The total occupancy of the *A'* site was constrained to unity in the refinement at 400 K.

Mn *L*<sub>2,3</sub>-edge XAS-MCD spectra for BiCu<sub>3</sub>Mn<sub>4</sub>O<sub>12</sub> at 9 K are shown in Fig. 4. The observed spectra correspond to *2p* → *3d* excitations of Cu and Mn. Both Cu *L*<sub>2</sub>- and *L*<sub>3</sub>-edge structures in the XAS spectra are single peaks, resembling those of Cu<sup>2+</sup> with *d*<sup>9</sup> electronic configuration and square-planar coordination, in CaCu<sub>3</sub>Ti<sub>4</sub>O<sub>12</sub>.<sup>14</sup> This suggests that Cu in BiCu<sub>3</sub>Mn<sub>4</sub>O<sub>12</sub> is divalent. The MCD intensities for the Cu *L*<sub>2</sub> and *L*<sub>3</sub> edges are evident, confirming that Cu<sup>2+</sup> spins at the *A'* sites are magnetically ordered. On the other hand, the Mn *L*<sub>2</sub>- and *L*<sub>3</sub>-edge structures do not resemble those of pure Mn<sup>3+</sup> or Mn<sup>4+</sup>, which is consistent with the averaged valence of 3.6+ for Mn calculated from the composition. Mn spins are also magnetically ordered from the MCD spectrum. An important observation here is that the signs of the MCD intensities of Cu *L* edges are opposite to those of the corresponding Mn *L* edges. This clearly demonstrates that the Cu and Mn spins are coupled antiferromagnetically. The total magnetic moment of Cu estimated from the XAS-MCD sum rules<sup>15-17</sup> was 1.16 μ<sub>B</sub>, which is in a good agreement with the value expected for divalent Cu. Here contribution from the magnetic dipole operator ⟨*T*<sub>*z*</sub>⟩ was neglected and the number of the Cu 3*d* electrons was assumed as 9. The magnetic moment of the Mn could not be evaluated from the XAS-MCD spectra because the *L*<sub>2</sub>- and *L*<sub>3</sub>-edge signals overlap.

The magnetic structure below *T*<sub>C</sub> was determined from the Rietveld analyses of the NPD patterns. The patterns from 5 to 400 K are shown in Fig. 5. Large increases in intensity were found in some reflections such as 020 and 022 below *T*<sub>C</sub>, corresponding to the evolution of the ordered magnetic moment. The absence of any additional reflection peaks to the *Im-3* symmetry indicates ferromagnetic alignment at both Cu and Mn sites. Considering the antiferromagnetic coupling of the Cu and Mn spins revealed by the XAS-MCD measure-

ments, the magnetic structure can be described as a ferrimagnetic order of Cu and Mn spins. Magnetic moments at both *A'* site (*M*<sub>*A'*</sub>) and *B* sites (*M*<sub>*B*</sub>) were refined for the patterns below 320 K. The result of the refinement of the pattern at 5 K is shown in Fig. 3 and summarized in Table I. Since the absolute orientation of the magnetic moments in a cubic structure cannot be determined by the NPD technique, both *M*<sub>*A'*</sub> and *M*<sub>*B*</sub> were set to the [001] direction in the refinements. *M*<sub>*A'*</sub> was found to be very small and could only be successfully refined at 5 and 100 K although there is no

TABLE II. Selected bond distances, bond angles, and BVS of BiCu<sub>2.4</sub>Mn<sub>4.6</sub>O<sub>12</sub> at 400, 300 and 5 K.<sup>a,b</sup>

	400 K	300 K	5 K
<i>d</i> (Bi-O) (Å) [×12]	2.598(2)	2.593(2)	2.589(2)
<i>d</i> (Cu <sub><i>A'</i></sub> /Mn <sub><i>A'</i></sub> -O) (Å) [×4]	1.953(1)	1.949(1)	1.948(1)
<i>d</i> (Cu <sub><i>A'</i></sub> /Mn <sub><i>A'</i></sub> -O) (Å) [×4]	2.743(2)	2.742(1)	2.737(2)
<i>d</i> (Cu <sub><i>A'</i></sub> /Mn <sub><i>A'</i></sub> -O) (Å) [×4]	3.233(1)	3.232(1)	3.225(1)
<i>d</i> (Mn <sub><i>B</i></sub> -O) (Å) [×6]	1.9429(3)	1.9415(4)	1.9380(3)
Cu-O-Cu (deg)	101.32(6)	101.28(6)	101.25(6)
Mn-O-Mn (deg)	141.24(6)	141.13(6)	141.20(6)
Cu-O-Mn (deg)	109.14(3)	109.19(3)	109.15(3)
BVS(Bi)	3.07	3.12	3.15
BVS(Cu <sub><i>A'</i></sub> )	2.19	2.22	2.22
BVS(Mn <sub><i>A'</i></sub> )	2.73	2.76	2.77
BVS(Mn <sub><i>B</i></sub> )	3.59	3.61	3.64

<sup>a</sup>BVS of Cu/Mn at the *A'* site BVS(Cu<sub>*A'*</sub>)/BVS(Mn<sub>*A'*</sub>) are both based on the average *A'*-O distances.

<sup>b</sup>The BVS parameters for trivalent/tetravalent Mn were used for Mn<sub>*A'*</sub>/Mn<sub>*B*</sub>.

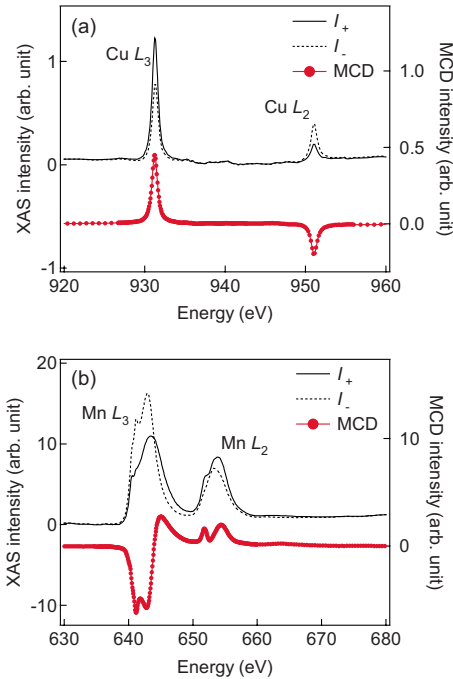


FIG. 4. (Color online) (a) Cu  $L_{2,3}$ -edges and (b) Mn  $L_{2,3}$ -edges XAS-MCD spectra for  $\text{BiCu}_{2.4}\text{Mn}_{4.6}\text{O}_{12}$  taken at 9 K. Solid ( $I_+$ ) and dashed ( $I_-$ ) lines show the XAS spectra measured with external field (2 T) applied parallel and antiparallel to the light propagation axis. The bottom line represents the MCD intensity ( $I_+ - I_-$ ).

magnetization evidence for a second magnetic transition below  $T_C$ . The refined magnetic moments for the two sites at 5 K were found to be parallel with values,  $M_{A'} = 0.24(4) \mu_B$  and  $M_B = 2.86(5) \mu_B$ , giving a total magnetic moment of  $M_{\text{tot}} = 12.2(3) \mu_B/\text{f.u.}$  The refined total magnetic moment seems to be considerably large compared to the observed magnetization of  $10.6 \mu_B/\text{f.u.}$  in the magnetic measurement. However, if we consider the off-stoichiometric composition and the amounts of impurities as we discussed before, the saturation magnetization is corrected to be  $12.1 \mu_B/\text{f.u.}$ ,<sup>18</sup> which is quite close to the refined value. Figure 6 shows the temperature dependence of the refined magnetic moments  $M_{A'}$ ,  $M_B$ , and  $M_{\text{tot}}$ . The thermal evolution of  $M_{\text{tot}}$  agrees well with the  $M/H$  behavior shown in Fig. 2.

The small positive value for  $M_{A'}$  appears anomalous considering the antiferromagnetic coupling between the  $A'$ -site Cu spins and the  $B$ -site Mn spins evidenced by MCD. This is most likely due to the presence of  $\text{Mn}^{3+}$  ions at the  $A'$  site. With the off-stoichiometric model  $\text{Bi}(\text{Cu}^{2+}_{0.8}\text{Mn}^{3+}_{0.2})_3\text{Mn}^{3.6+}_4\text{O}_{12}$  obtained above, the 80%  $\text{Cu}^{2+}$  ( $S=1/2$ ) and 20%  $\text{Mn}^{3+}$  ( $S=2$ ) spins at the  $A'$  sites each produce an ideal moment contribution of  $0.8 \mu_B$  per site. The observed average  $A'$ -site moment of  $\sim +0.2 \mu_B$  demonstrates an antiferromagnetic coupling of  $\text{Cu}^{2+}$  and  $\text{Mn}^{3+}$  moments at the  $A'$  sites, resulting in an almost complete cancellation of their moments. The lack of pure magnetic reflections indicates ferromagnetic alignment at each sublattices. Thus the magnetic structure can be described as

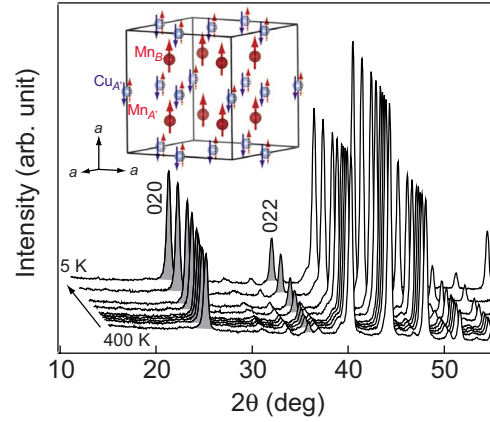


FIG. 5. (Color online) Thermal evolution of the low-angle region of the neutron powder-diffraction pattern of  $\text{BiCu}_{2.4}\text{Mn}_{4.6}\text{O}_{12}$ . Inset shows the magnetic structure below  $T_C$ .

illustrated in the inset of Fig. 5, where the  $A'$ -site  $\text{Cu}^{2+}$  spins couple antiferromagnetically with both the  $A'$ -site  $\text{Mn}^{3+}$  and the  $B$ -site  $\text{Mn}^{3.6+}$  spins. The saturation magnetization expected for  $\text{Bi}(\text{Cu}^{2+}_{0.8}\text{Mn}^{3+}_{0.2})_3\text{Mn}^{3.6+}_4\text{O}_{12}$  with such magnetic structure is  $13.6 \mu_B/\text{f.u.}$ , close to the measured one.

Since  $\text{Mn}_B$  in  $\text{BiCu}_{2.4}\text{Mn}_{4.6}\text{O}_{12}$  have mixed  $3+/4+$  oxidation states, a strong ferromagnetic double exchange interaction is expected as in other  $\text{AMnO}_3$  perovskites with mixed valence  $\text{Mn}^{3+/4+}$ , which should be responsible for the metallic conduction below  $T_C$ , as well as the large magnetoresistance. The ferromagnetic coupling between the  $A'$ - and  $B$ -site Mn spins suggests that some  $A'-B$  double exchange interactions also occur. The  $\text{Cu}^{2+}$  spins are localized and do not participate in the double exchange, and so couple through antiferromagnetic superexchange to their  $\text{Mn}_B$  neighbors. Direct  $\text{Cu}^{2+}-\text{Cu}^{2+}$  interaction in the  $A$ -site-ordered perovskites are very weak as the  $\text{CuO}_4$  square-planar units are separated from each other.<sup>3</sup> Hence the magnetism of  $\text{BiCu}_{2.4}\text{Mn}_{4.6}\text{O}_{12}$  is dominated by the strong ferromagnetic Mn-Mn and antiferromagnetic Cu-Mn interactions. The mixed  $3+/4+$  oxidation state in  $\text{Mn}_B$  and the ferrimagnetic coupling between the  $A'$ -site Cu and  $B$ -site Mn produce a half metallic electronic structure, where only up-spin bands cross the Fermi level below  $T_C$ . The spin-polarized conduction carriers are responsible for the large magnetoresistance in  $\text{BiCu}_{2.4}\text{Mn}_{4.6}\text{O}_{12}$ .

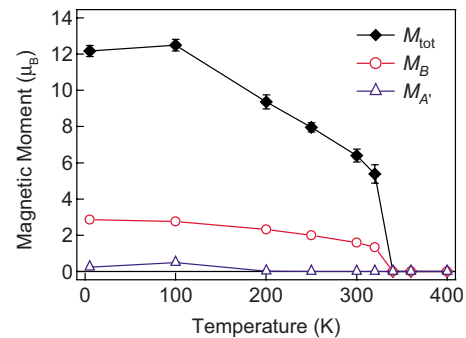


FIG. 6. (Color online) Temperature variation in the ordered magnetic moments for  $A'$  site ( $M_{A'}$ ) and  $B$  site ( $M_B$ ), and the total magnetic moment per formula unit ( $M_{\text{tot}}$ ).

## IV. CONCLUSIONS

The cation off-stoichiometry and magnetic order within the A-site-ordered double perovskite  $\text{BiCu}_3\text{Mn}_4\text{O}_{12}$  have been established using NPD and MCD spectroscopy. Off-stoichiometry originated from the substitution of  $\text{Mn}^{3+}$  for  $\text{Cu}^{2+}$  at the A' sites, leading to the chemical composition of  $\text{Bi}(\text{Cu}^{2+}_{0.8}\text{Mn}^{3+}_{0.2})_3\text{Mn}^{3.6+}_4\text{O}_{12}$ , as confirmed by the XAS spectroscopy and BVS calculations. A ferrimagnetic ordering between the A'-site  $\text{Cu}^{2+}$  and B-site  $\text{Mn}^{3+/4+}$  spins was obtained from the MCD and NPD experiments with the  $\text{Mn}^{3+/4+}$  and  $\text{Cu}^{2+}$  spins ordering simultaneously at  $T_C$ . However, the antiparallel alignment of  $\text{Mn}^{3+}$  and  $\text{Cu}^{2+}$  moments at the A' sites results in a very small net moment. The magnetism of the compound is dominated by the strong ferromagnetic Mn-Mn and antiferromagnetic Cu-Mn interactions.

## ACKNOWLEDGMENTS

We thank P. E. Car and Y. Ikeda for the assistance with the sample preparation, and P. Henry for the help in the data collection at ILL. We also thank M. Azuma for fruitful discussion. This work was partly supported by the Global COE Program (No. B09), Grants-in-Aid for Scientific Research (Grants No. 17105002, No. 19GS0207, No. 19014010, and No. 19340098), and a grant for the Joint Project of Chemical Synthesis Core Research Institutions from MEXT of Japan. The XAS experiments were performed with the approval of the Japan Synchrotron Radiation Research Institute (Grant No. 2008A-1001). The NPD experiments were done under the Strategic Japanese-UK Cooperative Program by JST/EPSCRC. Support was also provided by EPSCRC and the Leverhulme Trust, U.K.

\*Corresponding author; saito@scl.kyoto-u.ac.jp

- <sup>1</sup>M. Lufaso and P. M. Woodward, *Acta Crystallogr., Sect. B: Struct. Sci.* **57**, 725 (2001).
- <sup>2</sup>M. A. Subramanian, D. Li, N. Duan, B. A. Reisner, and A. W. Sleight, *J. Solid State Chem.* **151**, 323 (2000).
- <sup>3</sup>H. Shiraki, T. Saito, T. Yamada, M. Tsujimoto, M. Azuma, H. Kurata, S. Isoda, M. Takano, and Y. Shimakawa, *Phys. Rev. B* **76**, 140403(R) (2007).
- <sup>4</sup>W. Kobayashi, I. Terasaki, J. Takeya, I. Tsukuda, and Y. Ando, *J. Phys. Soc. Jpn.* **73**, 2373 (2004).
- <sup>5</sup>H. Shiraki, T. Saito, M. Azuma, and Y. Shimakawa, *J. Phys. Soc. Jpn.* **77**, 064705 (2008).
- <sup>6</sup>Z. Zeng, M. Greenblatt, M. A. Subramanian, and M. Croft, *Phys. Rev. Lett.* **82**, 3164 (1999).
- <sup>7</sup>J. A. Alonso, J. Sánchez-Benítez, A. D. Andrés, M. J. Martínez-Lope, M. T. Casais, and J. L. Martínez, *Appl. Phys. Lett.* **83**, 2623 (2003).
- <sup>8</sup>K. Takata, I. Yamada, M. Azuma, M. Takano, and Y. Shimakawa, *Phys. Rev. B* **76**, 024429 (2007).
- <sup>9</sup>A. C. Larson and R. B. Von Dreele, Los Alamos National Laboratory Report No. LAUR 86-748, 2004 (unpublished).
- <sup>10</sup>A. Prodi, E. Gilioli, A. Gauzzi, F. Licci, M. Marezio, F. Bolzoni, Q. Huang, A. Santoro, and J. W. Lynn, *Nature Mater.* **3**, 48 (2004).
- <sup>11</sup>Y. Long, T. Saito, M. Mizumaki, A. Agui, and Y. Shimakawa, *J. Am. Chem. Soc.* **131**, 16244 (2009).
- <sup>12</sup>Z. Zeng, M. Greenblatt, J. E. Sunstrom IV, M. Croft, and S. Khalid, *J. Solid State Chem.* **147**, 185 (1999).
- <sup>13</sup>D. Brown and D. Altermatt, *Acta Crystallogr., Sect. B: Struct. Sci.* **41**, 244 (1985).
- <sup>14</sup>C. McGuinness, J. E. Downes, P. Sheridan, P.-A. Glans, K. E. Smith, W. Si, and P. D. Johnson, *Phys. Rev. B* **71**, 195111 (2005).
- <sup>15</sup>P. Carra, B. T. Thole, M. Altarelli, and X. Wang, *Phys. Rev. Lett.* **70**, 694 (1993).
- <sup>16</sup>C. T. Chen, Y. U. Idzerda, H.-J. Lin, N. V. Smith, G. Meigs, E. Chaban, G. H. Ho, E. Pellegrin, and F. Sette, *Phys. Rev. Lett.* **75**, 152 (1995).
- <sup>17</sup>J. K. Freericks, T. P. Devereaux, M. Moraghebi, and S. L. Cooper, *Phys. Rev. Lett.* **94**, 216401 (2005).
- <sup>18</sup>The stoichiometric starting composition produces 87.1 wt %  $\text{BiCu}_{2.4}\text{Mn}_{4.6}\text{O}_{12}$ , 9.0 wt % CuO, and 3.9 wt %  $\text{Bi}_2(\text{CO}_3)\text{O}_2$ . The saturated magnetization of  $\text{BiCu}_{2.4}\text{Mn}_{4.6}\text{O}_{12}$  (molar weight=806.20 g/mol) is corrected with the assumption of those amounts of impurities.